World Journal of Gastroenterology

Submit a Manuscript: http://www.wjgnet.com/esps/
Help Desk: http://www.wjgnet.com/esps/helpdesk.aspx
DOI: 10.3748/wjg.v22.i37.8334

World J Gastroenterol 2016 October 7; 22(37): 8334-8348
ISSN 1007-9327 (print) ISSN 2219-2840 (online)
© 2016 Baishideng Publishing Group Inc. All rights reserved.

ORIGINAL ARTICLE

Basic Study

Characterisation of colonic dysplasia-like epithelial atypia in murine colitis

Sarron Randall-Demllo, Ruchira Fernando, Terry Brain, Sukhwinder Singh Sohal, Anthony L Cook, Nuri Guven, Dale Kunde, Kevin Spring, Rajaraman Eri

Sarron Randall-Demllo, Sukhwinder Singh Sohal, Dale Kunde, Rajaraman Eri, School of Health Sciences, University of Tasmania, Launceston, Launceston TAS 7250, Australia

Ruchira Fernando, Terry Brain, Department of Pathology, Launceston General Hospital, Launceston, Launceston TAS 7250, Australia

Anthony L Cook, Wicking Dementia Research and Education Centre, University of Tasmania, Hobart TAS 7005, Australia

Nuri Guven, Division of Pharmacy, School of Medicine, University of Tasmania, Hobart TAS 7005, Australia

Sukhwinder Singh Sohal, Breathe Well Centre of Research Excellence for Chronic Respiratory Disease and Lung Ageing, School of Medicine, University of Tasmania, Hobart TAS 7005, Australia

Kevin Spring, Medical Oncology, Ingham Institute for Applied Medical Research, Liverpool, Liverpool NSW 2170, Australia

Kevin Spring, Liverpool Clinical School, Western Sydney University, Richmond NSW 2753, Australia

Kevin Spring, South West Sydney Clinical School, University of New South Wales, Sydney NSW 2052, Australia

Author contributions: Randall-Demllo S and Eri R conceived and designed the experiments; Randall-Demllo S performed experiments and collected data; Randall-Demllo S, Fernando R and Brain T analysed the data; Fernando R, Brain T, Sohal SS, Cook AL, Gueven N, Kunde D and Eri R contributed reagents and materials; Randall-Demllo S, Fernando R, Brain T, Sohal SS, Cook AL, Gueven N, Kunde D, Spring K and Eri R contributed to writing the manuscript.

Supported by a Clifford Craig Medical Research Trust project grant and Cancer Council Tasmania (to Eri R and Kunde D); a Bowel Cancer Funding Partners PhD scholarship generously funded by Rotary District 9830, Australian Rotary Health and the University of Tasmania (to Randall-Demllo S).

Institutional review board statement: The study was reviewed and approved by the University of Tasmania Institutional Review Board.

Institutional animal care and use committee statement: All procedures involving animals were reviewed and approved by the Institutional Animal Care and Use Committee of the University of Tasmania animal Ethics Committee. Ethics Committee Number: A13329.

Conflict-of-interest statement: No conflict of interest exists.

Data sharing statement: All data relevant to this study are included in the paper and its supporting information.

Open-Access: This article is an open-access article which was selected by an in-house editor and fully peer-reviewed by external reviewers. It is distributed in accordance with the Creative Commons Attribution Non Commercial (CC BY-NC 4.0) license, which permits others to distribute, remix, adapt, build upon this work non-commercially, and license their derivative works on different terms, provided the original work is properly cited and the use is non-commercial. See: http://creativecommons.org/licenses/by-nc/4.0/

Manuscript source: Invited manuscript

Correspondence to: Rajaraman Eri, DVM, PhD, School of Health Sciences, University of Tasmania, Launceston, Churchill Avenue, Launceston TAS 7250, Australia. rderi@utas.edu.au
Telephone: +61-3-62262999

Received: June 27, 2016
Peer-review started: June 28, 2016
First decision: July 29, 2016
Revised: August 15, 2016
Accepted: September 6, 2016
Article in press: September 6, 2016
Published online: October 7, 2016

Abstract

AIM

To determine if exacerbation of pre-existing chronic colitis in Winnie (*Muc2* mutant) mice induces colonic dysplasia.

METHODS

Winnie mice and C57BL6 as a genotype control, were administered 1% w/v dextran sulphate sodium (DSS) orally, followed by drinking water alone in week-long cycles for a total of three cycles. After the third cycle, mice were killed and colonic tissue collected for histological and immunohistochemical evaluation. Inflammation and severity of dysplasia in the colonic mucosa were assessed in H&E sections of the colon. Epithelial cell proliferation was assessed using Ki67 and aberrant β-catenin signalling assessed with enzyme-based immunohistochemistry. Extracted RNA from colonic segments was used for the analysis of gene expression using real-time quantitative PCR. Finally, the distribution of Cxcl5 was visualised using immunohistochemistry.

RESULTS

Compared to controls, Winnie mice exposed to three cycles of DSS displayed inflammation mostly confined to the distal-mid colon with extensive mucosal hyperplasia and regenerative atypia resembling epithelial dysplasia. Dysplasia-like changes were observed in 100% of Winnie mice exposed to DSS, with 55% of these animals displaying changes similar to high-grade dysplasia, whereas high-grade changes were absent in wild-type mice. Occasional penetration of the muscularis mucosae by atypical crypts was observed in 27% of Winnie mice after DSS. Atypical crypts however displayed no evidence of oncogenic nuclear β-catenin accumulation, regardless of histological severity. Expression of *Cav1*, *Trp53* was differentially regulated in the distal colon of Winnie relative to wild-type mice. Expression of *Myc* and *Ccl5* was increased by DSS treatment in Winnie only. Furthermore, increased *Ccl5* expression correlated with increased complexity in abnormal crypts. While no overall difference in *Cxcl5* mucosal expression was observed between treatment groups, epithelial Cxcl5 protein appeared to be diminished in the atypical epithelium.

CONCLUSION

Alterations to the expression of *Cav1*, *Ccl5*, *Myc* and *Trp53* in the chronically inflamed Winnie colon may influence the transition to dysplasia.

Key words: Mice; Mucin-2; Colon; Colitis; Dysplasia; Dextran sulphate sodium

© The Author(s) 2016. Published by Baishideng Publishing Group Inc. All rights reserved.

Core tip: Patients with ulcerative colitis (UC) are at increased risk of developing colonic cancer. Understanding progression to early dysplastic change in the UC-associated inflammation in the colon required a suitable animal model. Winnie mice develop a UC-like chronic colitis and endoplasmic reticulum stress due to a *Muc2* mutation encoding a misfolded mucin-2. We hypothesised that exacerbation of pre-existing chronic inflammation using colitogenic dextran sulphate sodium in a model of spontaneous colitis would induce colorectal tumourigenesis. This study demonstrated that exacerbation of colitis resulted in epithelial hyperplasia in the distal colon and crypt abnormalities resembling dysplasia. Altered expression of genes known to modify tumour growth, specifically *Cav1*, *Ccl5*, *Myc* and *Trp53*, in *Muc2* mutants may predispose to early neoplastic change in the inflamed colon.

Randall-Demllo S, Fernando R, Brain T, Sohal SS, Cook AL, Guven N, Kunde D, Spring K, Eri R. Characterisation of colonic dysplasia-like epithelial atypia in murine colitis. *World J Gastroenterol* 2016; 22(37): 8334-8348 Available from: URL: http://www.wjgnet.com/1007-9327/full/v22/i37/8334.htm DOI: http://dx.doi.org/10.3748/wjg.v22.i37.8334

INTRODUCTION

Ulcerative colitis (UC) is a life-long immune disorder that presents as a chronic remitting and relapsing inflammation of the colon, which is also associated with an increased risk of colorectal cancer. Furthermore, the likelihood of developing cancer in the chronically inflamed colon is increased by both the duration and histologic severity of the inflammation[1,2]. Although the association between chronic colitis and colorectal cancer is well-known, the underlying mechanisms have yet to be defined, and due to the heterogeneous nature of the disease, a range of animal models are required to replicate the various aspects of its pathogenesis.

The origins of the chronic inflammation associated with UC may lie in an intrinsic defect in the secreted mucus barrier that lines the colonic surface epithelium. Disruption to the organisation of the colonic mucus, allows the penetration of bacteria into the normally uncolonised inner mucus layer adjacent to the surface epithelium, and possibly deeper into the crypts themselves[3]. Similar permeability defects are observed in patients with active UC, where bacterial-sized material penetrates the normally impenetrable inner mucus layer, a defect which, in a small subset of patients, may remain unimproved during remission[3].

The organised, meshwork-like structure of the secreted colonic mucus in both mice and humans is predominantly formed by the gel-forming mucin-2 (MUC2 and Muc2 in humans and mice respectively). Homozygous *Muc2* gene deletion abolishes Muc2 synthesis and the formation of a sterile inner colonic mucus layer, making Muc2-deficient animals susceptible to colitis caused by colonisation of the colonic mucosa by both pathogenic and normally

commensal bacterial species[4,5]. Homozygous *Muc2* deletion abrogates the formation of a protective colonic mucus initiating a chronic inflammation of the colonic mucosa similar to that observed in UC[6]. While Muc2-deficient mice have demonstrated the importance of Muc2-based mucus in preventing colitis, homozygous *Muc2* deletion is unlikely to reflect the nature of mucus abnormalities observed in UC. The colonic mucus in patients with UC while reduced in thickness, and though it remains penetrable by the luminal microbiota during active disease, the mucus layer is not totally abolished[3,7]. In this regard, the *Muc2* mutation of Winnie may better represent the situation in the inflamed colon of patients with UC. In Winnie mice, missense mutation of an N-terminal domain in *Muc2*, results in abnormal oligomerisation of Muc2 and a diminished colonic mucus secretion[8]. Aberrant Muc2 in Winnie also undergoes misfolding and accumulates within the goblet cell, triggering endoplasmic reticulum (ER) stress and activation of the unfolded protein response (UPR). Activation of the UPR and markers of ER-stress in the colonic epithelium has also been observed in patients with both active and inactive UC[8-10]. The combination of a defect in mucus secretion and concomitant ER-stress makes the Winnie mouse an interesting experimental model of the pathogenesis of UC. Unlike Muc2-deficient mice however, no incident of colonic neoplasia has yet been reported in Winnie mice.

While itself not a tumour suppressor gene, the protective function provided by the gel-forming mucin Muc2 is also necessary to prevent tumourigenesis in the large bowel. Homozygous Muc2 deletion in mice (C57BL6/J × 129SvOla background) has been associated an increased incidence of tumours in the small intestine, colon and rectum over a twelve-month span[11]. Distinct from the Muc2-deficient genotype described previously, the Winnie strain of mice also develop a spontaneous colitis due to Muc2 mutation.

We hypothesised that the defective mucus layer and resulting chronic colitis in Winnie would increase the incidence of colonic neoplasia. However, given the mild inflammation observed in the $Muc2^{-/-}$ and the low incidence of colonic tumours at twelve months, we intended to aggravate the existing inflammation in Winnie to accelerate the process of tumourigenesis. To accomplish this, we employed dextran sulphate sodium (DSS), widely used to induce colonic inflammation in normal (wild-type) and susceptible mouse strains. Administered in a cyclic pattern, DSS-induced inflammation can be used to promote neoplasia in mice already possessing initiating mutations in tumour suppressor genes such as those encoding APC/β-catenin, or p53[12-14] and alone may be sufficient to increase the incidence of colonic dysplasia and carcinoma in certain mouse strains[15,16]. Here we describe a dysplasia-like pathology of the distal colon in Winnie mice after three cycles of DSS administration.

MATERIALS AND METHODS

Ethics statement

All animal procedures were performed in accordance with the Australian Code of Practice for the Care and Use of Animals for Scientific Purposes of the National Health and Medical Research Council. The study was approved by the Animal Ethics Committee of the University of Tasmania (protocol #13329).

Animals

Eleven to twelve week-old Winnie mice (homozygous Muc2 mutant; C57BL6/J background) and age-matched C57BL/6J (Muc2 wild-type) mice of both sexes were used in this study. Animals were housed within individually ventilated cages containing a corncob bedding (Andersons, Maumee, OH, United States), in a room with a temperature maintained at 21 ℃, with a 12 h photoperiod. Mice were allowed access to radiation-sterilised rodent feed (Barastoc Rat and Mouse, Ridley AgProducts, Australia) and autoclaved tap water *ad libitum*.

Exacerbation of colitis with dextran sulphate sodium

Colitis was exacerbated though the oral administration of a 40000-50000 Da DSS (USB, Affymetrix Inc., Cleveland, OH, United States) through the drinking water. Stock solutions of DSS were prepared by dissolving DSS in sterile tap water and delivered in autoclaved water bottles at a concentration of 1% DSS (w/v). Pairs of Winnie and C57BL6J littermates were randomly allocated to one of two groups. A group of 12 Winnie and 6 C57BL6/J mice received 1% DSS dissolved in drinking water, whereas a control group of 6 Winnie and 4 C57BL6/J animals, was administered sterile drinking water only as a vehicle control. Each cycle of the experimental DSS regimen consisted of the administration of DSS for seven days before substitution of 1% DSS for water for an additional seven days. Mice in the experimental group received DSS in a total of three cycles over 42 d, with a single Winnie mouse euthanased prior to the conclusion of the DSS regimen. Mouse body weight and disease symptoms (*e.g.,* diarrhoea, rectal bleeding) were monitored daily during the experiment. During the course of the experiment one mouse displayed excessive weight loss and morbidity following the first DSS cycle and required euthanasia. At the day of experimental termination (day 42), all animals were killed *via* CO_2 asphyxiation before the abdomen was dissected and the colon removed.

Histopathological evaluation of colitis

The length of the colon from ileocaecal junction to the rectum was recorded. The colon was subsequently opened along its longitudinal axis and the luminal contents were removed prior to weighing the organ. The colon was bisected longitudinally and one half was prepared using the Swiss roll technique described

by[15], whereas the remaining colonic tissue was dissected and snap-frozen for molecular analyses. Swiss rolls 24 h fixation in 10% (v/v) neutral-buffered formalin. Swiss rolls were subsequently transferred to 70% ethanol prior to progressive dehydration, clearing and infiltration with HistoPrep paraffin wax (Fisher Scientific, Philadelphia, PA, United States). Swiss rolls were then embedded in wax and 5 μm sections cut at least three levels 50 μm apart using a rotary microtome. Sections were stained with haematoxylin and eosin Y (H&E; HD Scientific, Sydney, Australia). Slides stained with H&E were evaluated for inflammatory features and neoplasia. Histological inflammation was graded in a blinded fashion by SRD based on previously used criteria[16]. Briefly, crypt architectural distortion was graded 0-5, frequency of crypt abscesses graded 0-3, crypt hyperplasia graded 0-4, extent of mucosal damage graded 0-4, goblet cell depletion graded 0-4, extent of inflammatory infiltration graded 0-4 and frequency of lamina propria neutrophils graded 0-3. The inflammation score for each individual region (distal, middle and proximal colon) was derived from the sum of the score for each of the aforementioned criteria. Dysplastic change and submucosal invasion were graded as no change, low-grade dysplasia, high-grade dysplasia and invasive carcinoma. Crypts involved in glandular profunda were classified as non-dysplastic lesions. Assessment of dysplasia was performed independently by two pathologists (RF and TB) blinded to experimental groupings.

Immunohistochemistry

Slides were dewaxed and exposed to heat-induced epitope retrieval (4 min at 121 ℃) in a 10 mmol/L sodium citrate buffer, pH 6.0 in a decloaking chamber (Biocare Medical, Concord, CA, United States). Slides were cooled to room temperature and washed in 0.1 mol/L Tris-buffered saline (TBS) for 2 min per wash. Endogenous peroxidase activity was blocked by incubating slides in 3% H_2O_2 in methanol for 20 min, followed by 3 × 2 min washes (twice with dH_2O, followed by one wash with TBS). Background sniper (Biocare Medical) was applied to the slides for 20 min and washed off with 3 × 2 min washes with TBS. Slides were incubated with either anti-human β-catenin (clone E247; Abcam, Cambridge, United Kingdom), at a 1:500 dilution, rabbit anti-human Ki67 (clone SP6; Abcam) or rabbit anti-mouse Cxcl5 (Bioss Inc., Woburn, MA, United States) at a dilution of 1:100 was incubated with the slides for 1 h. Excess primary antibody was removed with 3 × 2 min washes with TBS prior to application of HRP-conjugated anti-rabbit secondary antibody (Biocare Medical) for 30 min. Slides were thoroughly rinsed with TBS for 3 × 2 min washes before the addition of a diaminobenzidine (DAB) chromagen solution (Biocare Medical) for 4 min. Tissue was subsequently counterstained with haematoxylin, dehydrated and mounted with DPX mountant (Sigma-Aldrich, Sydney, Australia). Slides were examined through an Olympus IX71 microscope (Olympus Australia, Melbourne, Australia) and images captured using the attached DP21 microscope camera (Olympus).

RNA extraction and RT-qPCR

Colonic tissue was homogenised using rotor-stator generator probes (Omni Scientific) and RNA extracted using the RNeasy Mini spin column kit (Qiagen, Melbourne, Australia) according to the manufacturer's instructions. To minimise genomic DNA contamination DNAse I (Qiagen) digestion was performed during the RNA extraction. Integrity and concentration of extracted RNA was assessed using the Experion Eukaryotic Total RNA electrophoretic system (Bio-Rad Laboratories). Samples with an RNA integrity number (RIN) > 7 were deemed suitable for RT-qPCR. Complementary DNA (cDNA) was synthesised from RNA samples using the iScript Reverse Transcription enzyme and reagents (Bio-Rad) using reaction conditions suggested by the manufacturer. Two-hundred nanograms of cDNA from each sample was added to a PCR reaction including TaqMan Fast Master Mix (Applied Biosystems, Foster City, CA, United States) and a single gene-specific TaqMan probe/primer set. Thermal cycling was performed using a StepOnePlus RT-qPCR instrument (Applied Biosystems). Primer sets used are specified in (Supplementary Table 1). Gene expression was quantified using the comparative ($\Delta\Delta C_T$) method where the threshold cycle (C_T) for each gene was normalised to reference gene *Gapdh*[17]. Relative gene expression in the DSS-treated animals was presented as $2^{-\Delta CT}$.

Statistical analysis

Change in body weight over time was compared using repeated-measures analysis of variance (ANOVA). Incidences of graded histological lesions were compared between treatment groups stratified within genotype using the Mantel-Haenszel χ^2 statistic. Comparisons between means of each unique combination of genotype and treatment were performed using a two-way ANOVA model. Differences in histological scores between anatomical regions were tested post-ANOVA using Tukey's multiple pairwise comparisons test. Non-parametric Spearman's rank correlation was used to test for monotonic relationships between relative transcript abundance and dysplasia scores (non-dysplastic = 1, low-grade = 2, high-grade = 3, dysplasia with submucosal component = 4). In all cases, a *P* value less than 0.05 were deemed to be statistically significant.

RESULTS

Clinical observations

Throughout the experiment, mice were monitored

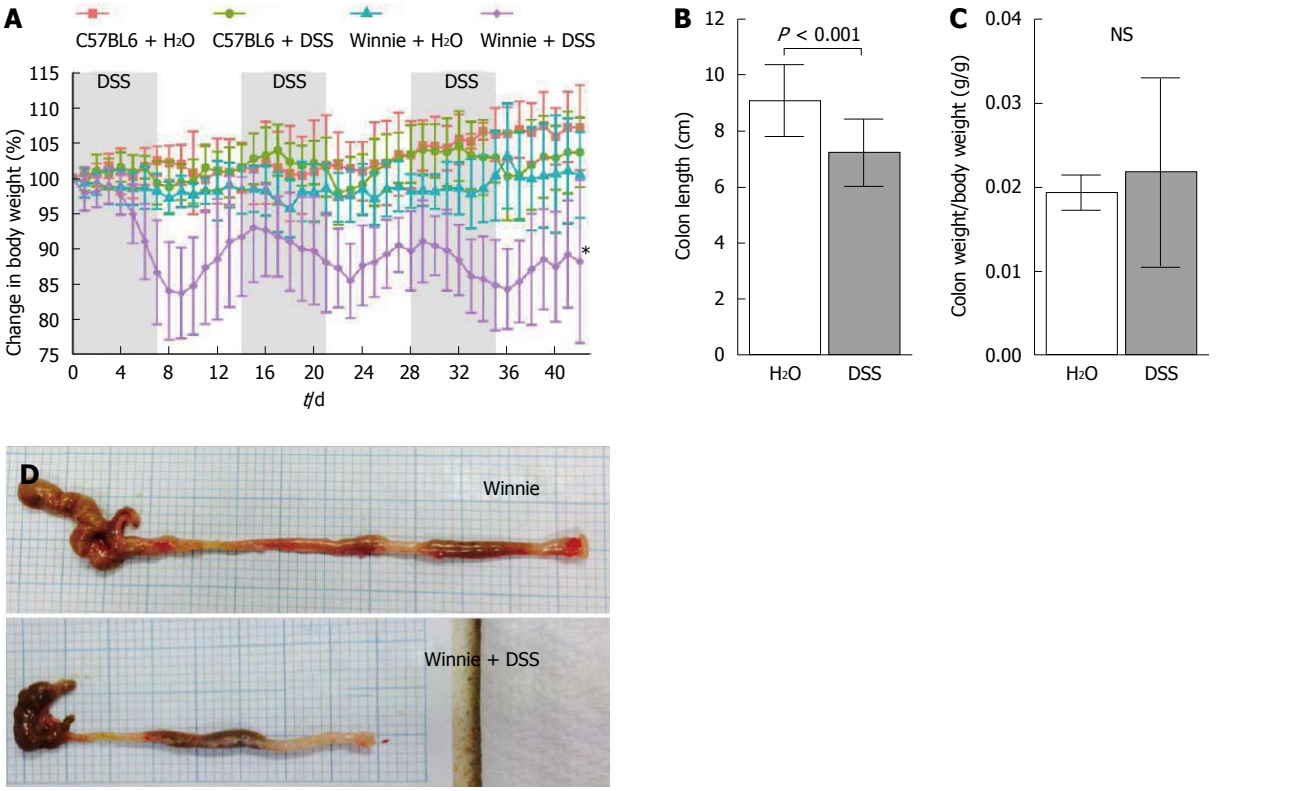

Figure 1 Clinical features of dextran sulphate sodium-induced colitis in Winnie. A: Daily change in body weight of wild-type; B: Winnie mice during the three cycle experimental dextran sulphate sodium (DSS) regimen. Body weight was recorded each day and recorded as percentage change from the starting body weight prior to commencement of the experiment (day 0). Each point represents the mean percentage change in body weight relative to the initial body weight (n = 4). Error bars depict standard deviation (SD) from the mean. Asterisk signifies difference (P < 0.05) between control Winnie mice and Winnie mice exposed to DSS; C: Mean colon length at termination. Error bars depict SD from the mean; D: Gross appearance of the Winnie colon at termination. Representative images of Winnie colon after receiving three cycles of water only (top) and the colon of Winnie receiving three cycles of DSS (bottom).

for the clinical symptoms of colitis. Prior to DSS administration individual Winnie mice of twelve weeks of age, displayed a mild, episodic, non-watery diarrhoea often accompanied by slight loss of body weight, which was usually resolved in 24 h. Clinical symptoms of colitis in eighteen week-old Winnie mice receiving water only did not differ discernibly from those exhibited at twelve weeks of age. Body weight in the control group, on average, remained stable, throughout the experiment (Figure 1A). Compared to the wild-type C57BL6/J, Winnie mice were more sensitive to the administration of DSS in the drinking water. DSS at 1% w/v for 7 d was sufficient to induce a bloody, watery diarrhoea accompanied by considerable weight loss (Figure 1B), which continued 1-2 d after cessation of DSS administration. Colon length in Winnie mice exposed to the DSS regimen was decreased by an average of 24% compared to Winnie mice receiving drinking water alone (Figure 1C). In contrast, colonic tissue from Winnie mice administered DSS was, even when standardised to body weight was no heavier than Winnies receiving only drinking water (Figure 1D). Upon gross post-mortem examination at experimental termination on day 42, the colons of Winnie mice administered DSS remained noticeably inflamed, with an apparent whitening and thickening of the colonic wall, and enlargement of mesenteric lymph nodes compared to control Winnie mice (Figure 1E).

Histopathology

Histological examination of the colon was undertaken to characterise the pathology induced by DSS in the Winnie colon. Initially the inflammation and mucosal damage induced by DSS in the Winnie colon was assessed. Cyclic DSS exacerbated the severity of inflammation in both middle and distal segments of Winnie mice relative to untreated Winnie mice, while DSS had only a minor influence on inflammation in the proximal colon (Figure 2). Compared to the wild-type C57BL6/J (Figure 3A) and wild-type exposed to three DSS cycles (Figure 3B), diffuse leukocytic infiltration into the mucosa, and to a lesser extent the submucosa, was common in the distal and mid-colon of Winnie mice (Figure 3C). In these mice, crypt architecture was occasionally irregular and frequently elongated, and infrequent crypt abscesses were observed. At the time of termination (day 42), severe damage to the distal and mid-colon of Winnie mice exposed to DSS remained evident (Figure 3D). DSS administration in Winnie resulted in an increased influx of leukocytes into the mucosa and submucosa. Large mucosal aggregates of mononuclear leukocytes were frequent, and often extended into the expanded submucosal compartment. Glandular profunda was

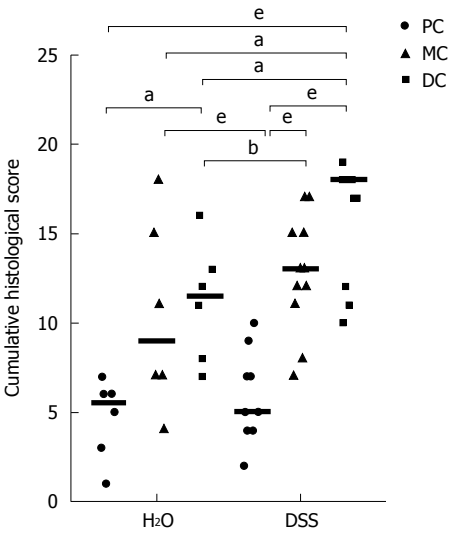

Figure 2 Three cycles of dextran sulphate sodium exacerbated Winnie colitis. Comparison of summed inflammation scores between control Winnie mice and Winnie mice receiving dextran sulphate sodium (DSS). PC, proximal colon, MC, middle colon, DC, distal colon. Bars represent medians of each group, individual animals represented as single points. $^{a}P < 0.05$, $^{b}P < 0.01$, $^{e}P < 0.001$.

occasionally observed in the distal colon involving the larger lymphoid aggregates, which expanded beyond the muscularis mucosae. Areas of superficial mucosal erosion and crypt loss were observed, frequently with foci of crypt fission adjacent the erosion (Figure 3D). Generally, the mucosa of the Winnie distal colon was extensively thickened and contained hyperplastic crypts following repeated DSS exposure. In addition to the typical inflammatory effects observed in Winnie, we assessed the colon for early neoplastic changes. Crypt hyperplasia within the distal and mid-colon of Winnie mice exposed to DSS was often accompanied by foci of abnormal crypt architecture resembling dysplasia. Forty-five percent of Winnie mice displayed crypt abnormalities consistent with a low-grade dysplasia after administration of DSS (Table 1), whereas aberrant crypts were only observed in one untreated Winnie mouse. Low-grade lesions displayed marked architectural distortion, with subtle cytological features such as crowding of epithelial nuclei and increased ratio of nucleus-to-cytoplasm (Figure 3D). Low-grade lesions were absent from all wild-type animals except for one of six C57BL6/J mice exposed to DSS (Table 1). High-grade lesions were observed in the middle and distal colon of 55% of Winnie mice exposed to DSS but were absent from the colon of untreated Winnie and all wild-type mice (Table 1). High-grade crypt lesions displayed the severe architectural distortions such as cribriform (Figure 4A and B) or back-to-back (Figure 4C and D) glandular arrangements associated with colonic dysplasia. In 27% of Winnie mice exposed to DSS, crypt epithelium could be observed within the submucosa underlying apparently dysplastic lesions separated by an intact muscularis mucosae (Table 1). Submucosal glands were lined

Table 1 Incidence and severity of dysplasia-like atypia

Group	Non-dysplastic	Low	High	Submucosal
C57BL/6J	4/4 (100%)	0/4 (0%)	0/4 (0%)	0/4 (0%)
C57BL/6J + DSS	5/6 (83%)	1/6 (17%)	0/6 (0%)	0/6 (0%)
Winnie	5/6 (83%)	1/6 (17%)	0/6 (0%)	1/6 (17%)
Winnie + DSS	0/11 (0%)	5/11 (45%)	6/11 (55%)	3/11 (27%)

Incidence of graded histological lesions in the distal colon of wild-type C57BL/6 and Winnie mice administered three cycles of DSS. Crypt lesions were graded as either non-dysplastic, low-grade or high-grade dysplasia and dysplasia with submucosal extension. The maximum grade observed was recorded for each animal. The incidence of dysplasia-like lesions in Winnie mice was increased by administration of DSS (Mantel-Haenszel $\chi^2 = 6.667$, $P < 0.01$).

with columnar or flattened cuboidal enterocytes but displayed minimal nuclear atypia (Figure 4A-D). Serial sections demonstrated continuity between abnormal mucosal glands and those in the submucosa. No obvious stromal reaction was associated with the submucosal glands. Notably, submucosal glands were usually observed in close proximity to the submucosal vasculature and mirrored the laterally spreading growth pattern seen in the mucosa.

Goblet cell hyperplasia was rare, occurring in a single animal in the Winnie group exposed to DSS (Figure 4C and D). Within a hyperplastic mucosal lesion with apparently high-grade architectural aberrations and mucus-retention cysts, hyperplastic goblet cells were observed in numerous crypts of lengths > 1 mm in length (Figure 4C).

Epithelial cell proliferation in the Winnie colon

Since colonic dysplasia may be associated with abnormal proliferation of the crypt epithelium we assessed the localisation of the Ki67 marker of proliferating cells. Normal Ki67-labelling in C57BL6/J mice extended uniformly for approximately a third of the crypt's total length (Figure 5A). Three cycles of 1% DSS in C57BL6 mice produced a slight expansion of the proliferative zone in the distal colon (Figure 5B). In contrast, the proliferative zone of the colonic crypt was expanded to approximately half to two-thirds of the total crypt length in Winnie mice (Figure 5C). Chronic exacerbation of colitis with DSS extended the Ki67-reactive proliferative zone toward the surface epithelium further than that typically seen in Winnie. Dysplasia-like lesions in Winnie displayed diffuse Ki67 labelling throughout the crypt length (Figure 5D). Notably, the base of some mucosal crypts contained a diffuse pattern of proliferative cells, a feature common to glands penetrating into the submucosa.

Beta-catenin localisation in the Winnie colon

To assess whether oncogenic perturbations in epithelial Wnt/β-catenin signalling were present in the chronically inflamed mucosa, we analysed the intracellular distribution of β-catenin immunohistochemically.

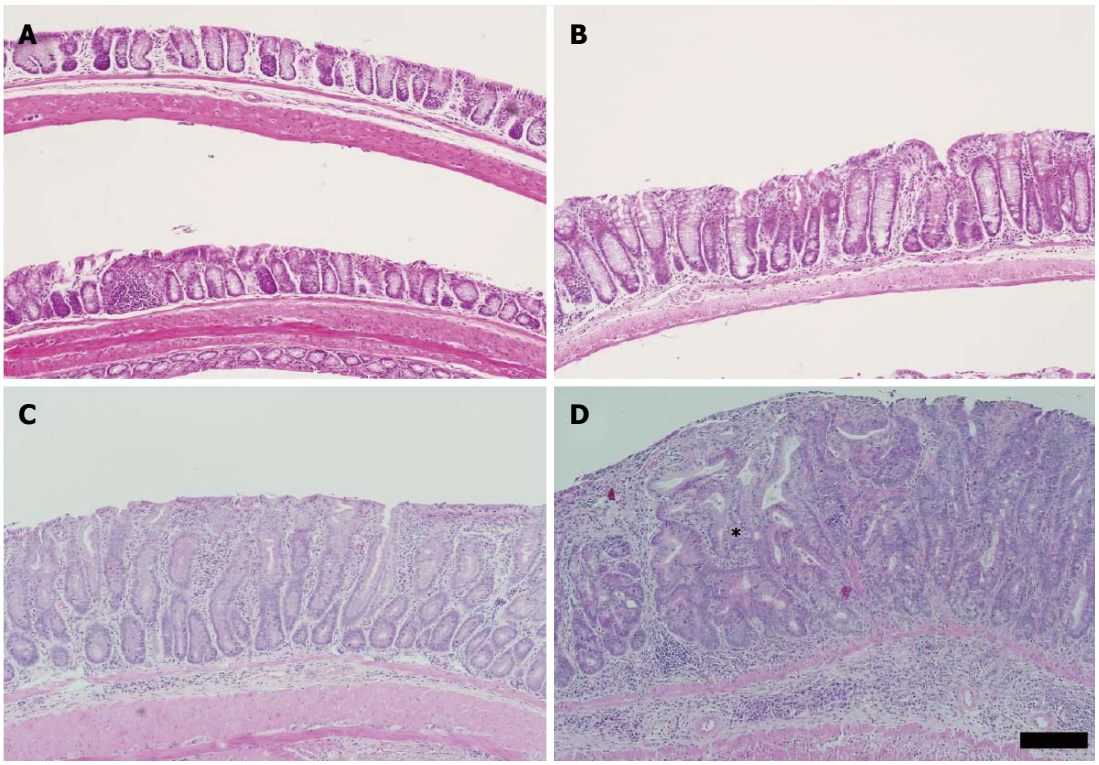

Figure 3 Distal colonic mucosal alterations induced by three cycles of dextran sulphate sodium. A: Representative image of the distal colon obtained from one of four untreated C57BL/6 mouse; B: C57BL/6 distal colon exposed to dextran sulphate sodium (DSS). Image representative of six eighteen week-old C57BL/6 mice exposed to three cycles of 1% DSS; C: Distal colon of Winnie mouse without exposure to DSS. Crypts are hyperplastic and the mucosa displays a marked leukocytic infiltration. Image representative of six untreated Winnie mice examined; D: Distal colon of Winnie mouse displaying colonic hyperplasia and mild focal dysplasia following three cycles of 1% DSS. Mucosa displays features of an active chronic inflammation, with prominent submucosal leukocytic infiltrate. Extensive crypt hyperplasia is visible with a focus of atypical glandular architecture (asterisk). Note the loss of surface epithelium. Numerous mitotic figures are evident. Image representative of the hyperplasia and dysplastic foci total of eleven Winnie mice exposed to three cycles of 1% DSS. All sections stained with H&E, scale bar is equivalent to 100 μm.

Localisation of β-catenin in the colonic mucosa of Winnie mice was restricted to the cell membrane of epithelial cells, and was visible to a lesser extent in the cytoplasm of epithelial cells (Figure 6A). Distribution of β-catenin was also predominantly membranous in Winnie mice following chronic exacerbation of colitis with DSS (Figure 6B). No nuclear translocation of β-catenin was evident in any of the dysplasia-like lesions in Winnie mice after DSS administration.

Gene expression analysis

To investigate potential mechanisms resulting in an abnormal epithelial regenerative or dysplastic response, we quantified transcription of a panel of genes associated with carcinogenesis. Included in our analysis were genes likely to accumulate in the chronically inflamed mucosa with known pro-tumourigenic effects such as cyclooxygenase-2 (*Ptgs2)* and interleukin-6 (*Il6*), and the chemokines *Ccl5*, *Cxcl5* and *Cxcl12*[18-20]. Other genes implicated in both inflammation and carcinogenesis included *Spp1* and *Vim*[21,22]. Central regulators of cellular proliferation and survival (*Cdkn2a, Myc* and *Trp53)*, cellular adhesion (*Cav1*), metabolism (*Pparg)*, cell surface glycoproteins (*Muc1* and *Prom1*), all of which have been implicated in cancers were also analysed[23-27]. Relative abundance of transcript for each gene varied considerably within individual mice with DSS-induced colitis, particularly in Winnie mice (Figure 7). Of the genes analysed, those encoding caveolin-1 (*Cav1*), C-C-motif-containing chemokine ligand 5 (*Ccl5*), myelocytomatosis oncogene (*Myc*) and the murine transformation-related protein p53 (*Trp53*), displayed significant alterations to expression in DSS-treated animals. Transcription of *Cav1* was altered by DSS in a manner that was dependent on the mouse strain. While *Cav1* expression in wild-type C57BL6 mice was increased by cyclic administration of 1% DSS, no increase in *Cav1* expression was observed between control Winnie mice and Winnie mice exposed to DSS. While *Ccl5* was unaltered between untreated Winnie and wild-type animals, DSS treatment increased *Ccl5* expression in Winnie relative to C57BL6 exposed to DSS. Expression of Myc in the distal colon was increased only in wild-type mice after the repeated administration of DSS whereas the same treatment had no observed effect on *Myc* expression in Winnie. Expression of *Trp53* was higher in Winnie mice than in the wild-type, but the DSS regimen did not produce a detectable effect on *Trp53* transcription in either wild-type or Winnie. The existence of a potential relationship between the relative abundance of the measured mRNA transcript in the distal colon of pooled Winnie and

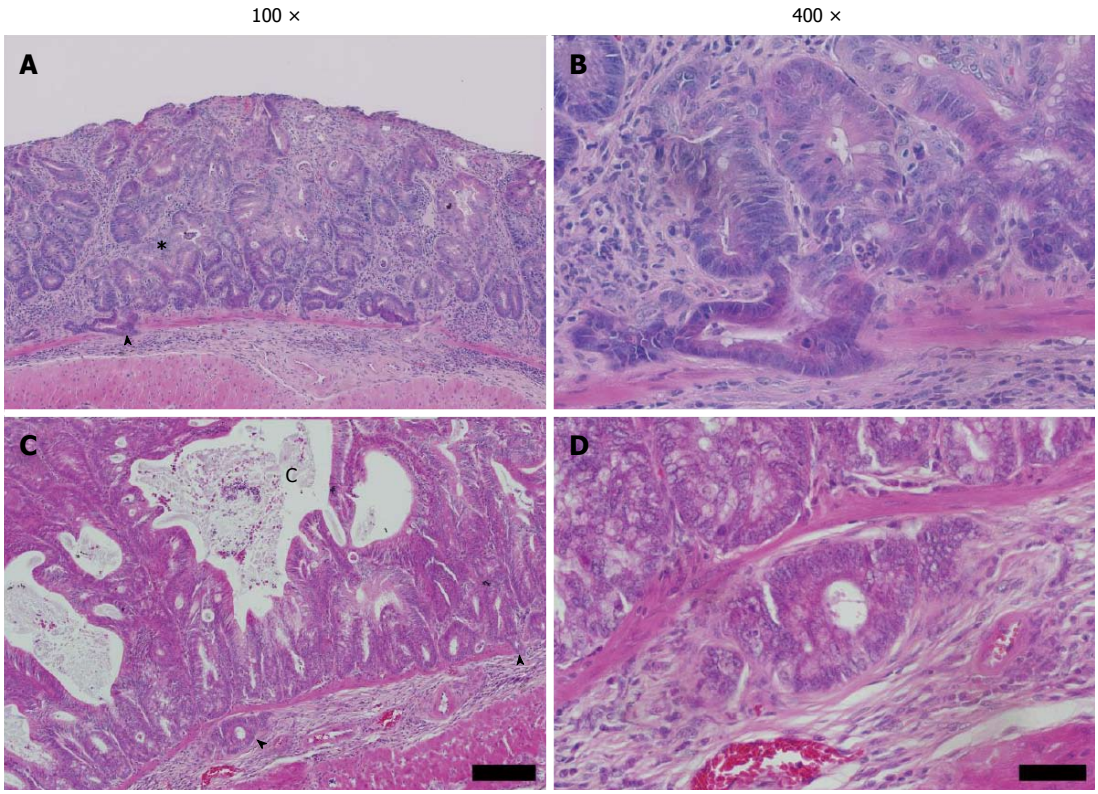

Figure 4 High-grade dysplasia and submucosal penetration in Winnie. A: Winnie distal colonic mucosa after DSS exposure. Distorted and atypical hyperplastic glands (asterisk), with focal infiltration into underlying submucosa through an otherwise intact muscularis mucosae (arrowhead); B: Higher magnification of A. Atypical mucosal and submucosal glands display relatively bland cytology; nuclear polarity mostly intact, though nucleus : cytoplasm ratio is increased. Mitotic figures are common beyond the crypt base. Region of crypt epithelium displaying loss of nuclear polarity (arrowheads). Note the stroma surrounding submucosal glands; C: Regenerative distal colonic mucosa featuring abnormal hyperplastic crypts. Multiple large mucus-containing cysts have formed, apparently formed by confluent dilated crypts lined with hyperplastic goblet cells. Crypts displayed back-to-back arrangement associated with high-grade dysplasia; D: Higher magnification of E. Focal penetration of the submucosa by atypical mucosal crypt. Multifocal penetration of the muscularis mucosae by the overlying abnormal crypts (arrowheads). Stained with HE, scale bar represents 100 μm in A and C, 20 μm in B and D.

Table 2 Spearman's correlation between mRNA transcript abundance and dysplasia severity

Gene	Restimate	*P* value
Cav1	-0.19	0.34
Ccl5	0.46	0.017[a]
Cdkn2a	0.11	0.61
Cxcl5	0.29	0.15[a]
Cxcl12	0.022	0.92
Il6	0.27	0.20
Muc1	-0.13	0.52
Myc	-0.26	0.20
Pparg	0.18	0.39
Prom1	0.18	0.39
Ptgs2	0.18	0.42
Spp1	0.40	0.049
Trp53	0.15	0.47
Vim	-0.14	0.51

Relationship between relative mRNA abundance (ΔΔCT) and severity of dysplasia in the distal colon was tested using Spearman's rank correlation. Estimate of Spearman's co-efficient of correlation (ρ) and corresponding *P* value for each gene are given, [a]$P < 0.05$.

C57BL6/J mice and the grade of dysplasia was tested using Spearman's rank correlation (Table 2). Monotonic increases in the gene expression of *Ccl5* (ρ = 0.46) and *Spp1* (ρ = 0.40) were weakly correlated with increasing severity of dysplasia. All other genes tested displayed no discernible statistical association between gene expression and histological severity.

Cxcl5 localisation in the Winnie colon

Given the large variance in increased abundance of Cxcl5 mRNA in the distal colon lysates, we sought to investigate the source and distribution of the Cxcl5 protein within colonic tissue. Immunolabelling of Cxcl5 protein revealed an altered pattern of expression subsequent to induction of colitis (Figure 8). Wild-type mice displayed a relatively low level of Cxcl5 in the colon, with cytoplasmic staining visible in colonic epithelial cells only. Cxcl5 production also appeared to be increased in the epithelial cells approaching the crypt apex when compared to epithelial cells located near the crypt base. Administration of 1% (w/v) DSS solution to C57BL6/J mice resulted in a slight increase in Cxcl5-specific staining in the crypt epithelium. Similarly, colitis induced by the Muc2 mutation in Winnie mice was associated with an increase in Cxcl5 protein levels within the intestinal epithelium. Additional insult of 1% DSS in Winnie mice produced

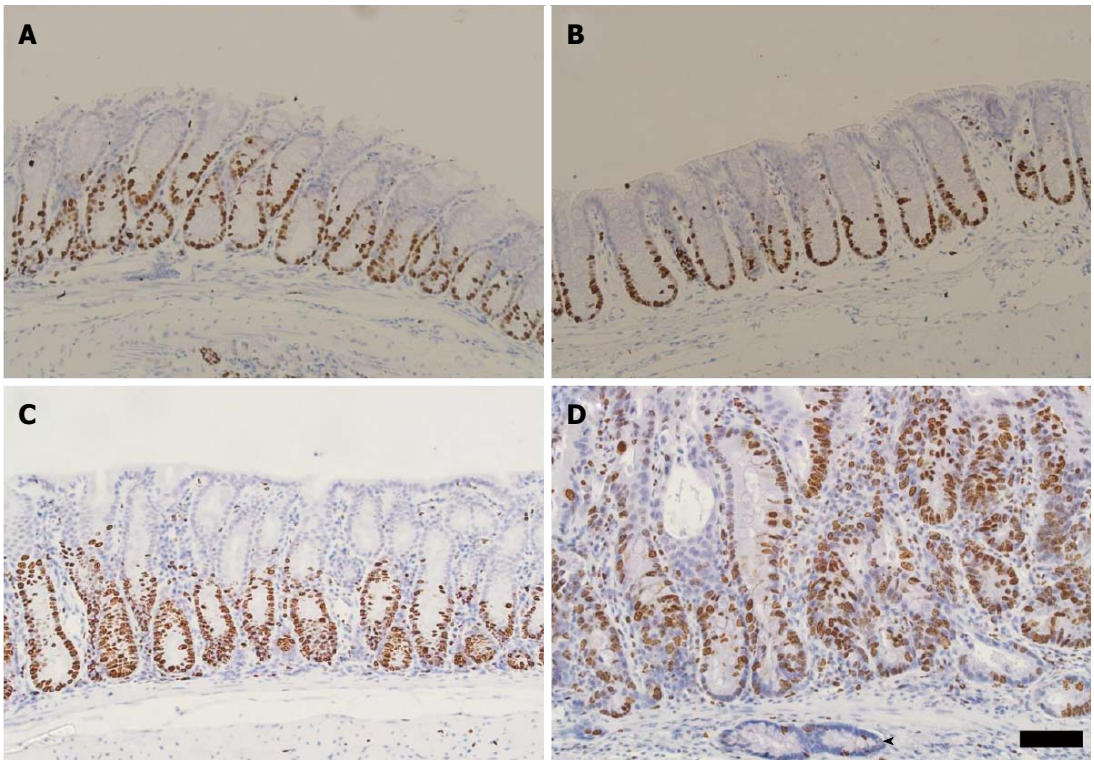

Figure 5 Immunohistochemical detection of Ki67 in Winnie distal colonic mucosa. A: Immunostaining of Ki67 in the distal colon of untreated C57BL6 mice. Image representative of Ki67 localisation in the distal colon of the four C57BL6 mice examined; B: Distal colonic Ki67 localisation representative of six C57BL6 mice exposed to three cycles of 1% dextran sulphate sodium (DSS); C: Distal colon of Winnie mouse without exposure to three cycles of DSS. Ki67-labelling in the epithelium is visible apically approximately half the crypt length; D: Ki67 immunolabelling of the Winnie distal colon exposed to three cycles of DSS. Crypt base proliferative zone extends approximately two-thirds of the crypt length. Submucosal gland (arrowhead) displays few positive nuclei. Scale bar represents a distance of 50 μm.

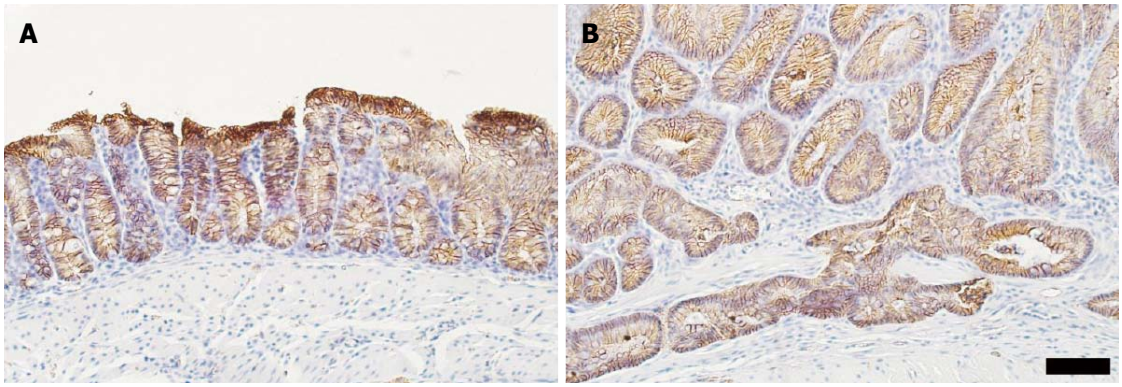

Figure 6 Localisation of β-catenin in Winnie distal colonic mucosa. A: Representative image of Winnie distal colon of the six animals without DSS exposure immunostained for β-catenin. B-catenin in the colonic epithelium is primarily associated with the epithelial cell membrane; B: Immunostained dysplastic distal colonic mucosa from a Winnie mouse exposed to three cycles of DSS (representative of *n* = 11). B-catenin localised to the cell membrane of epithelial cells without any nuclear accumulation. Scale bar is equivalent to 100 μm.

still higher levels of Cxcl5 in the intestinal epithelium. Notably the production of Cxcl5 was also increased in mucosal and submucosal leukocytes.

DISCUSSION

The pathology of UC is associated with a depletion of the protective colonic mucus layer, suggesting a reduction in mucus secretion from colonic goblet cells[7]. Experimental evidence suggests however, that a partial reduction in mucin secretion may be insufficient to permit the development of colitis[28]. Disruption of the normal colonic mucus structure through Muc2 ablation or altered post-translational modification, permeabilises the normally impenetrable inner mucus layer to bacteria[3]. A similar permeabilisation of the colonic mucus was observed in the inflamed colonic mucosa of UC patients, suggesting that Muc2 mutation may

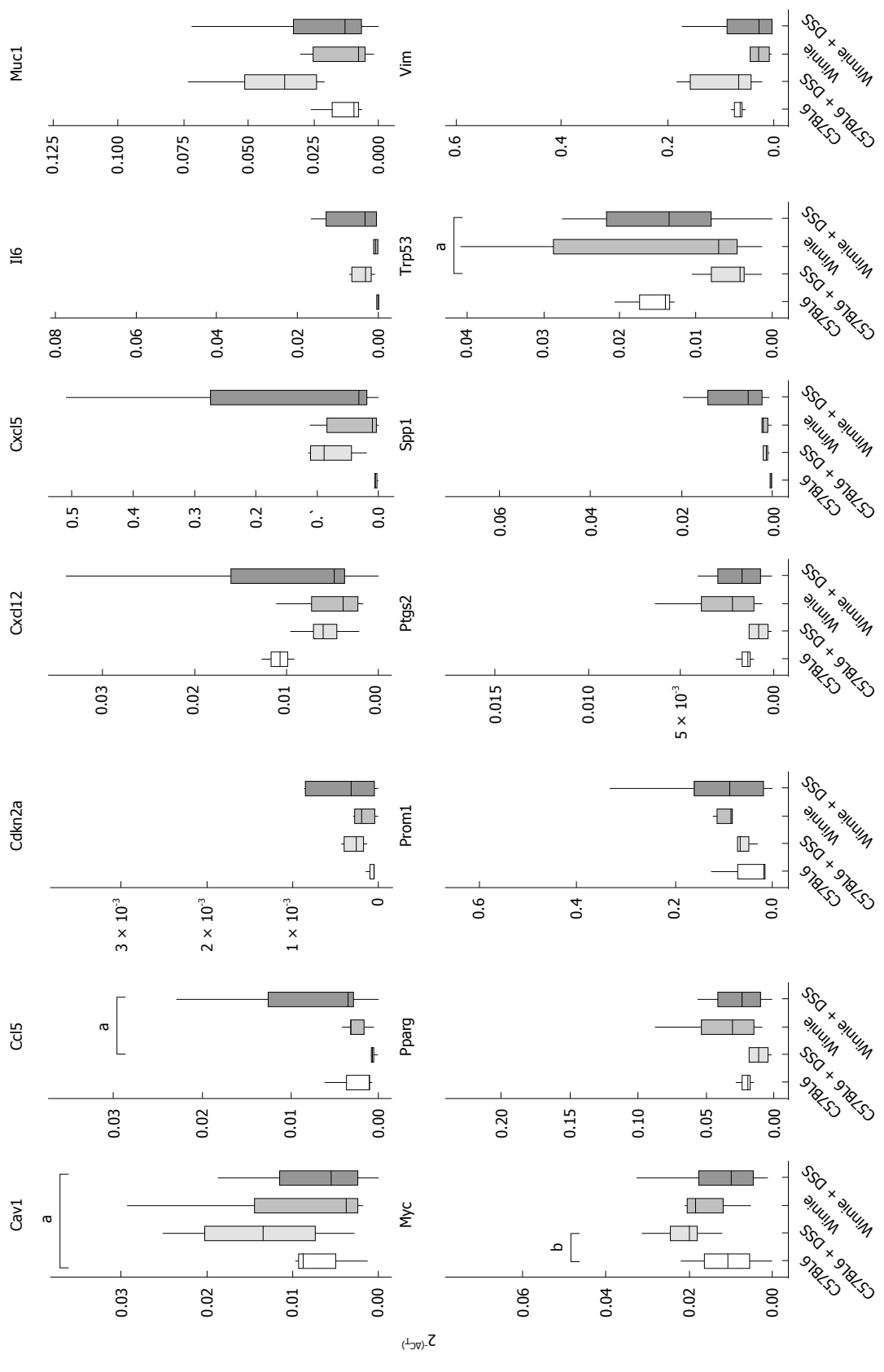

Figure 7 Relative transcript abundance of genes regulating inflammation and cell proliferation. Transcript abundance measured from 25 ng of template based on the linearised 2-ΔCT method, where each gene of interest was normalised to the relative abundance of a reference gene (Gapdh). Box plot depicts interquartile range (IQR) either side of the median for each combination of treatment and genotype (3-11 mice per group). Whiskers represent 1.5 IQR approximately equivalent to 5%-95% confidence intervals. $^{a}P < 0.05$, $^{b}P < 0.01$.

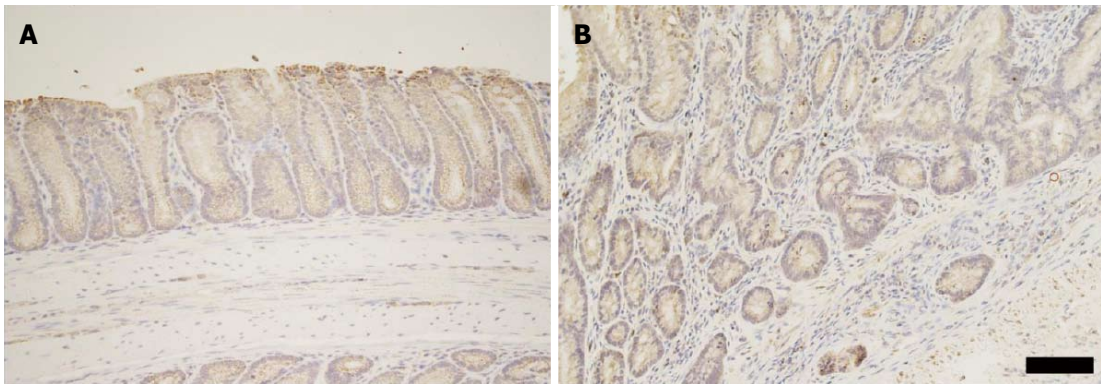

Figure 8 Immunohistochemical detection of Cxcl5 in Winnie distal colonic mucosa A. Representative distal colon from Winnie without DSS exposure (*n* = 6). Cxcl5 labelling displayed a diffuse cytoplasmic pattern in the colonic epithelium; B. Representative distal mucosa of Winnie exposed to DSS (*n* = 11). Dysplastic glands displaying focal reduction in epithelial Cxcl5. Weak Cxcl5 immunolabelling is present within the cytoplasm of the epithelial cells lining dysplastic glands. Note that submucosal epithelium penetrating the muscularis mucosae retains Cxcl5 expression. Scale bar represents 50 μm.

simulate this aspect of UC pathology[3,29]. Mice with a homozygous deletion of *Muc2* demonstrate several key pathological differences to UC. Muc2-deficient mice display relatively normal goblet cell numbers and a compensatory increase in other mucins such as Muc6, features which are not observed in UC[10]. Increasing evidence also points to possible intrinsic defects in protein synthesis and prolonged ER stress in the colonic epithelium affected by UC[8,9]. Since Winnie mice display spontaneous chronic colitis with an impaired mucus barrier and concomitant epithelial ER stress, they may provide an informative model for the pathogenesis of UC-associated inflammation and neoplasia.

Based on the Muc2 mutant mouse, the expected colonic tumours in Winnie mice could only be infrequent even at twelve months of age, limiting its utility as an experimental model of colonic carcinogenesis. We therefore provided further insult to the colon using DSS, to further disrupt the integrity of the mucus barrier. Consistent with its ability to permeabilise the inner colonic mucus layer, Winnie mice were more sensitive to 1% DSS than Muc2 wild-type C57BL6 mice. Acute administration of DSS produced mucosal injury characterised by superficial erosion and prominent inflammatory infiltrates containing neutrophils and macrophages among other leukocytes[30]. Much of this tissue damage remained at the end of the three cycles of DSS in Winnie mice with areas of mucosal erosion interspersed between regions of hypertrophic mucosa in the distal half of the colon. Notably, Winnie mice that received DSS displayed an increased frequency of abnormal crypt foci resembling dysplasia. Pre-cancerous epithelial dysplasia has been previously reported in the distal colon of Swiss Webster mice exposed to DSS[15,31]. While DSS appeared to rapidly produce foci of non-polypoid dysplasia in the distal colon of 100% Winnie mice under our experimental conditions, the neoplastic potential of these lesions remains uncertain. The time-frame used in the present study is considerably shorter than that used by Cooper *et al*[15] and incident lesions in Winnie could be expected to be less advanced. Penetration of crypt epithelium into the submucosa was observed in 27% of Winnie mice exposed to DSS as opposed to 17% and 0% in the control Winnie group and both C57BL/6 groups respectively. Minimal fibrosis was observed surrounding the laterally spreading submucosal glands and were frequently associated with small breaches of the muscularis mucosae. Such crypts were usually cytologically bland, negative for β-catenin nuclear accumulation and contained a small population of proliferating cells. The close proximity of glands entering the submucosa to blood and lymphatic vessels perhaps suggests that infiltrate the submucosa through weak points in the muscularis mucosae through which these vessels pass. Study of later time-points post-DSS administration would provide evidence as to whether laterally spreading crypts infiltrating the submucosa underlie the rapid progression of colitis-associated neoplasms.

Given the difficulty of identifying possible malignancy in the regenerative mucosa, we subsequently examined the mucosa of the distal colon for molecular features indicative of pre-neoplastic transformation. Hyperactivation of β-catenin signalling is an event associated with the pre-cancerous polyps in 46% of sporadically occurring adenomatous dysplasia[32]. Nuclear translocation of membrane-associated β-catenin is normally limited by the ubiquitinylating activity of the APC-GSK3β-Axin-complex, thereby preventing excessive enhancement of cyclin-D1 and c-myc transcription[33-35]. Tumourigenic Apc/β-catenin mutation may result in the accumulation of active β-catenin protein in the nucleus, which are detectable immunohistochemically[36]. Apparently dysplastic lesions in Winnie lacked the cytoplasmic and nuclear redistribution of β-catenin associated with pre-neoplastic transformation. Induction of dysplasia and neoplasia in mice using DSS alone highlighted the differences in cancers arising from the flat mucosa opposed to those arising from polypoid lesions[15]. Dysplasia/carcinoma

in flat lesions in 94% of cases, displayed membranous localisation of β-catenin whereas evidence of nuclear β-catenin was detected in all polypoid lesions. Studies of DSS-induced neoplasia are concordant with those in human UC-associated neoplasms. Nuclear β-catenin in UC-associated carcinoma is infrequent compared to sporadic cases, presumably due to the low incidence of Apc or β-catenin mutations[32,37].

Gene expression in the distal colon of Winnie revealed altered expression of p53 (*Trp53*), a central regulator of various stress responses. Frequent *TP53* gene mutations in IBD-associated neoplasms and their occurrence prior to dysplasia in patients with UC indicates the importance of the gene in preventing carcinogenesis[38]. An accumulation of mutagenic reactive oxygen and nitrogen species in the mucosa may cause these initial mutations in *TP53* and potentially other genes[38]. Although the presence of mutations was not assessed, *Trp53* transcription was increased in Winnie, even without exposure to DSS, perhaps indicative of DNA damage accrued from prolonged oxidative stress. Alternatively, the differential transcription *Trp53* in Winnie may imply that the chronic ER stress and activation of the unfolded protein response (UPR) due to misfolded Muc2[39]. Since Myc is subject to transcriptional regulation via Wnt/β-catenin signalling, alterations to Myc expression are observed in colonic carcinogenesis[34]. Oncogenic alterations to Myc presumably interfere with normal Myc-dependent regulation of cell proliferation, apoptosis and cellular metabolism[24]. Up-regulation of *Myc* in wild-type mice post-DSS is consistent with reported increases in *Myc* mRNA in the mucosa of mice in patients with IBD[40,41]. It is unclear however, why a similar increase in *Myc* mRNA was absent in Winnie mice exposed to DSS. Further study into the known interactions between *Myc* and chronic activation of the PERK/eIF2α-mediated UPR pathway in Winnie may explain the different responses between genotypes[42]. Another modifier of carcinogenesis, caveolin-1 (*Cav1*), was also increased in wild-type animals post-DSS. Caveolin-1 is scaffolding protein that regulates the transduction of growth factor signalling and is thus capable of restraining external pro-proliferative signals in epithelial cells[25]. The effect of attenuated *Cav1* expression in the DSS-induced pathology of Winnie is unclear as caveolin-1 may be either under-expressed or over-expressed in colorectal cancers[43,44]. Analysis of the mutational status of *Apc* and Kras in the Winnie colonic mucosa may explain the expression level of caveolin-1[45,46].

Recruitment of leukocytes, particularly neutrophils to the colonic mucosa is a hallmark of the inflammation observed in Winnie. Consistent with the relatively large influx of leukocytes into the Winnie distal colonic mucosa and submucosa following DSS, expression of the chemokine *Ccl5* was increased. Increased Ccl5 production has been associated with ineffective lymphocytic anti-tumour responses[47]. Unlike the Gαi2$^{-/-}$ model of spontaneous colitis and colon cancer, we observed a correlation between dysplastic progression and increased Ccl5 expression[48]. Similarly, transcription of the pro-inflammatory cytokine *Spp1* also correlated with increasing severity of dysplasia.

The chemokine Cxcl5, like IL-8, contains a neutrophil-activating ELR domain and is capable of inducing neutrophil chemotaxis through the Cxcr2 chemokine receptor[49]. Unlike IL-8 however, which is produced predominantly by endothelial and myeloid-derived cells in the colon, CXCL5 is primarily produced by crypt epithelial cells. Synthesis of CXCL5 has been reported to increase in ulcerative colitis in humans, presumably prompted by direct exposure to bacterial pathogen-associated molecular patterns, or by the milieu of pro-inflammatory cytokines in the colonic mucosa[50]. Up-regulation of Cxcl5 is therefore likely important for the efficient phagocytosis of bacteria in humans and animals with an impaired colonic mucus barrier. Cxcl5 expression was observed to increase along with the progression of high-grade dysplastic lesions into invasive carcinoma. Relative to control animals, expression of Cxcl5 was considerably heterogeneous in the distal colon of Winnie mice exposed to DSS. Distribution of Cxcl5 expanded to mucosal leukocytes in the distal colon of Winnie mice after DSS exposure. Perhaps explaining the heterogeneity in Cxcl5 transcription, was the occurrence of crypt foci containing regions of epithelium expressing low levels of Cxcl5, though there was no obvious association between dysplasia and loss of Cxcl5. Despite the indications for increased Cxcl5 expression reflecting the progression of dysplasia to advanced colonic carcinoma[51,52]. In contrast, low levels of Cxcl5 expression have been associated with a more aggressive disease course in rat and human CRC cases[53]. Activation of nuclear factor-κB signalling is known to regulate the expression of both Cxcl5, therefore production of Cxcl5 could be dependent on paracrine signalling through the IL-1 receptor[50,54]. Further characterisation of cells within the abnormal glands would be required to gain an appreciation of the role of Cxcl5 in DSS-induced pathology.

In conclusion, chronic DSS exposure in mice with impaired colonic mucin secretion produced extensive mucosal hypertrophy in response to inflammation. Abnormal, dysplasia-like crypt foci were present within the hyperplastic mucosa and in several instances penetrated into the submucosa. Though no β-catenin accumulation was observed, the distal colon of Winnie mice displayed extensive epithelial proliferation and the differential expression of genes regulating epithelial cell proliferation and apoptosis (*Cav1*, *Myc* and *Trp53*) during recovery from DSS. Expression of leukocyte chemo-attractant *Ccl5* was increased in Winnie post-DSS and correlated with histological severity. Analysis of the involved pathways at further time points may yield further insight into the transition to dysplastic and cancerous colonic mucosa in the context of chronic colitis.

ACKNOWLEDGMENTS

The authors would like to thank the staff of the Pathology Department, Launceston General Hospital and Mr Dane Hayes for their guidance and technical assistance.

COMMENTS

Background

Patients with ulcerative colitis (UC) are at increased risk of developing CRC, and are prone to more aggressive tumour progression. Chronic inflammation and subsequent regeneration of the colonic mucosa is thought to initiate the formation of dysplastic precursors through mechanisms which are yet to be fully elucidated.

Research frontiers

Much of our knowledge regarding colitis-associated neoplasia comes from experimental models utilising genotoxic carcinogens. Few studies have also explored the effect of mucin depletion and concomitant ER stress on the initiation of neoplasia.

Innovations and breakthroughs

These results suggest that altered gene expression in the distal colon of Winnie mice relative to the wild-type may correspond to the crypt abnormalities in Winnie mice.

Applications

Further characterisation of the molecular pathways involved in the repair of the Winnie mucosa may be useful targets for future studies. Manipulation of the involved pathways in experimental models of chronic colitis may provide stronger evidence for a role in the transition from inflammation to neoplasia.

Terminology

Dysplasia: In the colon, refers to histological changes in both glandular architecture and cytology, specifically those associated with pre-cancerous molecular changes. Endoplasmic reticulum stress: Impairment of the ability of the endoplasmic reticulum to facilitate protein synthesis and folding results in the engagement of various molecular pathways which may induce autophagy and apoptosis. Neoplasia: Tissue which displays a dysregulated pattern of growth and dysplastic features, commonly presenting as tumours. Neoplasms that acquire the ability to invade and/or metastasise into separate tissue compartments are considered cancerous or 'malignant' neoplasms.

Peer-review

This is an interesting manuscript on the impact of colitis in MUC2 mutation Winnie mice (decreased mucus production). The understanding of this animal model may be useful in the understanding of severe colitis leading to dysplasia and tumorigenesis in ulcerative colitis.

REFERENCES

1 **Rutter MD**, Saunders BP, Wilkinson KH, Rumbles S, Schofield G, Kamm MA, Williams CB, Price AB, Talbot IC, Forbes A. Cancer surveillance in longstanding ulcerative colitis: endoscopic appearances help predict cancer risk. *Gut* 2004; **53**: 1813-1816 [PMID: 15542520 DOI: 10.1136/gut.2003.038505]

2 **Gupta RB**, Harpaz N, Itzkowitz S, Hossain S, Matula S, Kornbluth A, Bodian C, Ullman T. Histologic inflammation is a risk factor for progression to colorectal neoplasia in ulcerative colitis: a cohort study. *Gastroenterology* 2007; **133**: 1099-1105; quiz 1340-1341 [PMID: 17919486 DOI: 10.1053/j.gastro.2007.08.001]

3 **Johansson ME**, Gustafsson JK, Holmén-Larsson J, Jabbar KS, Xia L, Xu H, Ghishan FK, Carvalho FA, Gewirtz AT, Sjövall H, Hansson GC. Bacteria penetrate the normally impenetrable inner colon mucus layer in both murine colitis models and patients with ulcerative colitis. *Gut* 2014; **63**: 281-291 [PMID: 23426893 DOI: 10.1136/gutjnl-2012-303207]

4 **Johansson ME**, Phillipson M, Petersson J, Velcich A, Holm L, Hansson GC. The inner of the two Muc2 mucin-dependent mucus layers in colon is devoid of bacteria. *Proc Natl Acad Sci USA* 2008; **105**: 15064-15069 [PMID: 18806221 DOI: 10.1073/pnas.0803124105]

5 **Bergstrom KS**, Kissoon-Singh V, Gibson DL, Ma C, Montero M, Sham HP, Ryz N, Huang T, Velcich A, Finlay BB, Chadee K, Vallance BA. Muc2 protects against lethal infectious colitis by disassociating pathogenic and commensal bacteria from the colonic mucosa. *PLoS Pathog* 2010; **6**: e1000902 [PMID: 20485566 DOI: 10.1371/journal.ppat.1000902]

6 **Wenzel UA**, Magnusson MK, Rydstrom A, Jonstrand C, Hengst J, Johansson ME, Velcich A, Ohman L, Strid H, Sjovall H, Hansson GC, Wick MJ. Spontaneous colitis in Muc2-deficient mice reflects clinical and cellular features of active ulcerative colitis. *PLoS ONE* 2014; **9**: e100217

7 **Pullan RD**, Thomas GA, Rhodes M, Newcombe RG, Williams GT, Allen A, Rhodes J. Thickness of adherent mucus gel on colonic mucosa in humans and its relevance to colitis. *Gut* 1994; **35**: 353-359 [PMID: 8150346]

8 **Heazlewood CK**, Cook MC, Eri R, Price GR, Tauro SB, Taupin D, Thornton DJ, Png CW, Crockford TL, Cornall RJ, Adams R, Kato M, Nelms KA, Hong NA, Florin TH, Goodnow CC, McGuckin MA. Aberrant mucin assembly in mice causes endoplasmic reticulum stress and spontaneous inflammation resembling ulcerative colitis. *PLoS Med* 2008; **5**: e54 [PMID: 18318598 DOI: 10.1371/journal.pmed.0050054]

9 **Tréton X**, Pédruzzi E, Cazals-Hatem D, Grodet A, Panis Y, Groyer A, Moreau R, Bouhnik Y, Daniel F, Ogier-Denis E. Altered endoplasmic reticulum stress affects translation in inactive colon tissue from patients with ulcerative colitis. *Gastroenterology* 2011; **141**: 1024-1035 [PMID: 21699776 DOI: 10.1053/j.gastro.2011.05.033]

10 **Van der Sluis M**, De Koning BA, De Bruijn AC, Velcich A, Meijerink JP, Van Goudoever JB, Büller HA, Dekker J, Van Seuningen I, Renes IB, Einerhand AW. Muc2-deficient mice spontaneously develop colitis, indicating that MUC2 is critical for colonic protection. *Gastroenterology* 2006; **131**: 117-129 [PMID: 16831596 DOI: 10.1053/j.gastro.2006.04.020]

11 **Velcich A**, Yang W, Heyer J, Fragale A, Nicholas C, Viani S, Kucherlapati R, Lipkin M, Yang K, Augenlicht L. Colorectal cancer in mice genetically deficient in the mucin Muc2. *Science* 2002; **295**: 1726-1729 [PMID: 11872843 DOI: 10.1126/science.1069094]

12 **Tanaka T**, Kohno H, Suzuki R, Hata K, Sugie S, Niho N, Sakano K, Takahashi M, Wakabayashi K. Dextran sodium sulfate strongly promotes colorectal carcinogenesis in Apc(Min/+) mice: inflammatory stimuli by dextran sodium sulfate results in development of multiple colonic neoplasms. *Int J Cancer* 2006; **118**: 25-34 [PMID: 16049979 DOI: 10.1002/ijc.21282]

13 **Takahashi M**, Nakatsugi S, Sugimura T, Wakabayashi K. Frequent mutations of the beta-catenin gene in mouse colon tumors induced by azoxymethane. *Carcinogenesis* 2000; **21**: 1117-1120 [PMID: 10836998]

14 **Fujii S**, Fujimori T, Kawamata H, Takeda J, Kitajima K, Omotehara F, Kaihara T, Kusaka T, Ichikawa K, Ohkura Y, Ono Y, Imura J, Yamaoka S, Sakamoto C, Ueda Y, Chiba T. Development of colonic neoplasia in p53 deficient mice with experimental colitis induced by dextran sulphate sodium. *Gut* 2004; **53**: 710-716 [PMID: 15082590]

15 **Cooper HS**, Murthy S, Kido K, Yoshitake H, Flanigan A. Dysplasia and cancer in the dextran sulfate sodium mouse colitis model. Relevance to colitis-associated neoplasia in the human: a study of histopathology, B-catenin and p53 expression and the role of inflammation. *Carcinogenesis* 2000; **21**: 757-768 [PMID: 10753213]

16 **Inoue T**, Murano M, Kuramoto T, Ishida K, Kawakami K, Abe Y, Morita E, Murano N, Toshina K, Nishikawa T, Maemura

K, Shimamoto C, Hirata I, Katsu K, Higuchi K. Increased proliferation of middle to distal colonic cells during colorectal carcinogenesis in experimental murine ulcerative colitis. *Oncol Rep* 2007; **18**: 1457-1462 [PMID: 17982630]
17 **Livak KJ**, Schmittgen TD. Analysis of relative gene expression data using real-time quantitative PCR and the 2(-Delta Delta C(T)) Method. *Methods* 2001; **25**: 402-408 [PMID: 11846609 DOI: 10.1006/meth.2001.1262]
18 **Sheehan KM**, O'Connell F, O'Grady A, Conroy RM, Leader MB, Byrne MF, Murray FE, Kay EW. The relationship between cyclooxygenase-2 expression and characteristics of malignant transformation in human colorectal adenomas. *Eur J Gastroenterol Hepatol* 2004; **16**: 619-625 [PMID: 15167166]
19 **Chalaris A**, Schmidt-Arras D, Yamamoto K, Rose-John S. Interleukin-6 trans-signaling and colonic cancer associated with inflammatory bowel disease. *Dig Dis* 2012; **30**: 492-499 [PMID: 23108305 DOI: 10.1159/000341698]
20 **Lim JB**, Chung HW. Serum ENA78/CXCL5, SDF-1/CXCL12, and their combinations as potential biomarkers for prediction of the presence and distant metastasis of primary gastric cancer. *Cytokine* 2015; **73**: 16-22 [PMID: 25689618 DOI: 10.1016/j.cyto.2015.01.010]
21 **Wu XL**, Lin KJ, Bai AP, Wang WX, Meng XK, Su XL, Hou MX, Dong PD, Zhang JJ, Wang ZY, Shi L. Osteopontin knockdown suppresses the growth and angiogenesis of colon cancer cells. *World J Gastroenterol* 2014; **20**: 10440-10448 [PMID: 25132760 DOI: 10.3748/wjg.v20.i30.10440]
22 **Adegboyega PA**, Mifflin RC, DiMari JF, Saada JI, Powell DW. Immunohistochemical study of myofibroblasts in normal colonic mucosa, hyperplastic polyps, and adenomatous colorectal polyps. *Arch Pathol Lab Med* 2002; **126**: 829-836 [PMID: 12088453 DOI: 10.1043/0003-9985(2002)126<0829: ISOMIN>2.0.CO; 2]
23 **Risques RA**, Lai LA, Himmetoglu C, Ebaee A, Li L, Feng Z, Bronner MP, Al-Lahham B, Kowdley KV, Lindor KD, Rabinovitch PS, Brentnall TA. Ulcerative colitis-associated colorectal cancer arises in a field of short telomeres, senescence, and inflammation. *Cancer Res* 2011; **71**: 1669-1679 [PMID: 21363920 DOI: 10.1158/0008-5472.CAN-10-1966]
24 **Dang CV**. MYC on the path to cancer. *Cell* 2012; **149**: 22-35 [PMID: 22464321 DOI: 10.1016/j.cell.2012.03.003]
25 **Sotgia F**, Martinez-Outschoorn UE, Howell A, Pestell RG, Pavlides S, Lisanti MP. Caveolin-1 and cancer metabolism in the tumor microenvironment: markers, models, and mechanisms. *Annu Rev Pathol* 2012; **7**: 423-467 [PMID: 22077552 DOI: 10.1146/annurev-pathol-011811-120856]
26 **Beatty PL**, Plevy SE, Sepulveda AR, Finn OJ. Cutting edge: transgenic expression of human MUC1 in IL-10-/- mice accelerates inflammatory bowel disease and progression to colon cancer. *J Immunol* 2007; **179**: 735-739
27 **Sgambato A**, Corbi M, Svelto M, Caredda E, Cittadini A. New Insights into the CD133 (Prominin-1) Expression in Mouse and Human Colon Cancer Cells. *Adv Exp Med Biol* 2013; **777**: 145-166 [PMID: 23161081 DOI: 10.1007/978-1-4614-5894-4_10]
28 **Gregorieff A**, Stange DE, Kujala P, Begthel H, van den Born M, Korving J, Peters PJ, Clevers H. The ets-domain transcription factor Spdef promotes maturation of goblet and paneth cells in the intestinal epithelium. *Gastroenterology* 2009; **137**: 1333-1345.e1-3 [PMID: 19549527 DOI: 10.1053/j.gastro.2009.06.044]
29 **Laroui H**, Ingersoll SA, Liu HC, Baker MT, Ayyadurai S, Charania MA, Laroui F, Yan Y, Sitaraman SV, Merlin D. Dextran sodium sulfate (DSS) induces colitis in mice by forming nano-lipocomplexes with medium-chain-length fatty acids in the colon. *PLoS One* 2012; **7**: e32084 [PMID: 22427817 DOI: 10.1371/journal.pone.0032084]
30 **Perše M**, Cerar A. Dextran sodium sulphate colitis mouse model: traps and tricks. *J Biomed Biotechnol* 2012; **2012**: 718617 [PMID: 22665990 DOI: 10.1155/2012/718617]
31 **Okayasu I**, Yamada M, Mikami T, Yoshida T, Kanno J, Ohkusa T. Dysplasia and carcinoma development in a repeated dextran sulfate sodium-induced colitis model. *J Gastroenterol Hepatol* 2002; **17**: 1078-1083 [PMID: 12201867]
32 **Aust DE**, Terdiman JP, Willenbucher RF, Chang CG, Molinaro-Clark A, Baretton GB, Loehrs U, Waldman FM. The APC/beta-catenin pathway in ulcerative colitis-related colorectal carcinomas: a mutational analysis. *Cancer* 2002; **94**: 1421-1427 [PMID: 11920497]
33 **Tetsu O**, McCormick F. Beta-catenin regulates expression of cyclin D1 in colon carcinoma cells. *Nature* 1999; **398**: 422-426 [PMID: 10201372 DOI: 10.1038/18884]
34 **He TC**, Sparks AB, Rago C, Hermeking H, Zawel L, da Costa LT, Morin PJ, Vogelstein B, Kinzler KW. Identification of c-MYC as a target of the APC pathway. *Science* 1998; **281**: 1509-1512 [PMID: 9727977]
35 **Ikeda S**, Kishida S, Yamamoto H, Murai H, Koyama S, Kikuchi A. Axin, a negative regulator of the Wnt signaling pathway, forms a complex with GSK-3beta and beta-catenin and promotes GSK-3beta-dependent phosphorylation of beta-catenin. *EMBO J* 1998; **17**: 1371-1384 [PMID: 9482734 DOI: 10.1093/emboj/17.5.1371]
36 **Sheng H**, Shao J, Williams CS, Pereira MA, Taketo MM, Oshima M, Reynolds AB, Washington MK, DuBois RN, Beauchamp RD. Nuclear translocation of beta-catenin in hereditary and carcinogen-induced intestinal adenomas. *Carcinogenesis* 1998; **19**: 543-549 [PMID: 9600336]
37 **Mikami T**, Yoshida T, Numata Y, Kikuchi M, Araki K, Nakada N, Okayasu I. Invasive behavior of ulcerative colitis-associated carcinoma is related to reduced expression of CD44 extracellular domain: comparison with sporadic colon carcinoma. *Diagn Pathol* 2011; **6**: 30 [PMID: 21473743 DOI: 10.1186/1746-1596-6-30]
38 **Hussain SP**, Amstad P, Raja K, Ambs S, Nagashima M, Bennett WP, Shields PG, Ham AJ, Swenberg JA, Marrogi AJ, Harris CC. Increased p53 mutation load in noncancerous colon tissue from ulcerative colitis: a cancer-prone chronic inflammatory disease. *Cancer Res* 2000; **60**: 3333-3337 [PMID: 10910033]
39 **Thomas SE**, Malzer E, Ordóñez A, Dalton LE, van 't Wout EF, Liniker E, Crowther DC, Lomas DA, Marciniak SJ. p53 and translation attenuation regulate distinct cell cycle checkpoints during endoplasmic reticulum (ER) stress. *J Biol Chem* 2013; **288**: 7606-7617 [PMID: 23341460 DOI: 10.1074/jbc.M112.424655]
40 **Suzuki R**, Miyamoto S, Yasui Y, Sugie S, Tanaka T. Global gene expression analysis of the mouse colonic mucosa treated with azoxymethane and dextran sodium sulfate. *BMC Cancer* 2007; **7**: 84 [PMID: 17506908 DOI: 10.1186/1471-2407-7-84]
41 **Serafino A**, Moroni N, Zonfrillo M, Andreola F, Mercuri L, Nicotera G, Nunziata J, Ricci R, Antinori A, Rasi G, Pierimarchi P. WNT-pathway components as predictive markers useful for diagnosis, prevention and therapy in inflammatory bowel disease and sporadic colorectal cancer. *Oncotarget* 2014; **5**: 978-992 [PMID: 24657851 DOI: 10.18632/oncotarget.1571]
42 **Hart LS**, Cunningham JT, Datta T, Dey S, Tameire F, Lehman SL, Qiu B, Zhang H, Cerniglia G, Bi M, Li Y, Gao Y, Liu H, Li C, Maity A, Thomas-Tikhonenko A, Perl AE, Koong A, Fuchs SY, Diehl JA, Mills IG, Ruggero D, Koumenis C. ER stress-mediated autophagy promotes Myc-dependent transformation and tumor growth. *J Clin Invest* 2012; **122**: 4621-4634 [PMID: 23143306 DOI: 10.1172/JCI62973]
43 **Bender FC**, Reymond MA, Bron C, Quest AF. Caveolin-1 levels are down-regulated in human colon tumors, and ectopic expression of caveolin-1 in colon carcinoma cell lines reduces cell tumorigenicity. *Cancer Res* 2000; **60**: 5870-5878 [PMID: 11059785]
44 **Fine SW**, Lisanti MP, Galbiati F, Li M. Elevated expression of caveolin-1 in adenocarcinoma of the colon. *Am J Clin Pathol* 2001; **115**: 719-724 [PMID: 11345836 DOI: 10.1309/YL54-CCU7-4V0P-FDUT]
45 **Roy UK**, Henkhaus RS, Ignatenko NA, Mora J, Fultz KE, Gerner EW. Wild-type APC regulates caveolin-1 expression in human colon adenocarcinoma cell lines via FOXO1a and C-myc. *Mol Carcinog* 2008; **47**: 947-955 [PMID: 18444242 DOI: 10.1002/mc.20451]
46 **Basu Roy UK**, Henkhaus RS, Loupakis F, Cremolini C, Gerner

EW, Ignatenko NA. Caveolin-1 is a novel regulator of K-RAS-dependent migration in colon carcinogenesis. *Int J Cancer* 2013; **133**: 43-57 [PMID: 23280667 DOI: 10.1002/ijc.28001]

47 **Chang LY**, Lin YC, Mahalingam J, Huang CT, Chen TW, Kang CW, Peng HM, Chu YY, Chiang JM, Dutta A, Day YJ, Chen TC, Yeh CT, Lin CY. Tumor-derived chemokine CCL5 enhances TGF-β-mediated killing of CD8(+) T cells in colon cancer by T-regulatory cells. *Cancer Res* 2012; **72**: 1092-1102 [PMID: 22282655 DOI: 10.1158/0008-5472.CAN-11-2493]

48 **Götlind YY**, Fritsch Fredin M, Kumawat AK, Strid H, Willén R, Rangel I, Bland PW, Hörnquist EH. Interplay between T(h)1 and T(h)17 effector T-cell pathways in the pathogenesis of spontaneous colitis and colon cancer in the Gαi2-deficient mouse. *Int Immunol* 2013; **25**: 35-44 [PMID: 22962436 DOI: 10.1093/intimm/dxs089]

49 **Walz A**, Burgener R, Car B, Baggiolini M, Kunkel SL, Strieter RM. Structure and neutrophil-activating properties of a novel inflammatory peptide (ENA-78) with homology to interleukin 8. *J Exp Med* 1991; **174**: 1355-1362 [PMID: 1744577]

50 **Keates S**, Keates AC, Mizoguchi E, Bhan A, Kelly CP. Enterocytes are the primary source of the chemokine ENA-78 in normal colon and ulcerative colitis. *Am J Physiol* 1997; **273**: G75-G82 [PMID: 9252512]

51 **Kawamura M**, Toiyama Y, Tanaka K, Saigusa S, Okugawa Y, Hiro J, Uchida K, Mohri Y, Inoue Y, Kusunoki M. CXCL5, a promoter of cell proliferation, migration and invasion, is a novel serum prognostic marker in patients with colorectal cancer. *Eur J Cancer* 2012; **48**: 2244-2251 [PMID: 22197219 DOI: 10.1016/j.ejca.2011.11.032]

52 **Rubie C**, Frick VO, Wagner M, Schuld J, Gräber S, Brittner B, Bohle RM, Schilling MK. ELR+ CXC chemokine expression in benign and malignant colorectal conditions. *BMC Cancer* 2008; **8**: 178 [PMID: 18578857 DOI: 10.1186/1471-2407-8-178]

53 **Speetjens FM**, Kuppen PJ, Sandel MH, Menon AG, Burg D, van de Velde CJ, Tollenaar RA, de Bont HJ, Nagelkerke JF. Disrupted expression of CXCL5 in colorectal cancer is associated with rapid tumor formation in rats and poor prognosis in patients. *Clin Cancer Res* 2008; **14**: 2276-2284 [PMID: 18413816 DOI: 10.1158/1078-0432.ccr-07-4045]

54 **Dimberg J**, Dienus O, Löfgren S, Hugander A, Wågsäter D. Expression and gene polymorphisms of the chemokine CXCL5 in colorectal cancer patients. *Int J Oncol* 2007; **31**: 97-102 [PMID: 17549409]

P- Reviewer: Keely S, Lakatos PL, Toh JWT, Upala S
S- Editor: Qi Y **L- Editor**: A **E- Editor**: Wang CH